

# Coupled-channel study of $\gamma p \rightarrow K^+ \Lambda$

Wen-Tai Chiang<sup>a,b</sup>, F. Tabakin<sup>a</sup>

<sup>a</sup>*Department of Physics and Astronomy, University of Pittsburgh, PA 15260, USA*

<sup>b</sup>*Department of Physics, National Taiwan University, Taipei 10617, Taiwan*

T.-S. H. Lee<sup>c</sup>, B. Saghai<sup>d</sup>

<sup>c</sup>*Physics Division, Argonne National Laboratory, Argonne, IL 60439, USA*

<sup>d</sup>*Service de Physique Nucléaire, DAPNIA-DSM, CEA/Saclay, F-91191  
Gif-sur-Yvette, France*

---

## Abstract

A coupled-channel (CC) approach has been developed to investigate kaon photoproduction on the nucleon. In addition to direct  $K^+ \Lambda$  production, our CC approach accounts for strangeness production including  $K^+ \Lambda$  final state interactions with both  $\pi^0 p$  and  $\pi^+ n$  intermediate states. Calculations for the  $\gamma p \rightarrow K^+ \Lambda$  reaction have been performed, and compared with the recent data from SAPHIR, with emphasis on the CC effects. We show that the CC effects are significant at the level of inducing 20% changes on total cross sections; thereby, demonstrating the need to include  $\pi N$  channels to correctly describe the  $\gamma p \rightarrow K^+ \Lambda$  reaction.

*Key words:* Kaon photoproduction, Coupled channel, Final-state interaction, Meson-baryon interaction

*PACS:* 13.60.Le, 25.20.Lj, 11.80.Gw, 13.75.Jz

---

## 1 Introduction

A major issue in strong interaction physics is to understand baryon spectroscopy. Meson-baryon scattering has been the predominant reaction used to study the properties of nucleon resonances ( $N^*$ ). An appealing alternative is to use electromagnetic probes, e.g.,  $\gamma N \rightarrow N^* \rightarrow \pi N$ . In this photon-induced process, the relative weakness of the electromagnetic interaction allows one to use first-order descriptions of the incident channel, thus making possible more reliable extraction of  $N^*$  information from data. With the recent development of new facilities such as Jefferson Lab, ELSA, GRAAL, MAMI, and

SPring-8, it is now possible to obtain accurate data for meson electromagnetic production, including spin-dependent observables.

Among meson photoproduction processes, pion photoproduction is by far the most studied theoretically and experimentally. However, increased effort has also been devoted in recent years to investigate kaon photoproduction. Such studies are motivated by several considerations: (1) the production of strangeness associated with kaons ( $K$ ) and hyperons ( $Y$ ) allows one to study the role played by  $s$  quarks versus  $u$  and  $d$  quarks; (2) higher mass resonances can be better studied by investigating the  $N^* \rightarrow K\Lambda$  and  $N^* \rightarrow K\Sigma$  decays; (3) the so-called “missing resonances” [1,2] predicted by quark models, but not observed in  $\pi N$  scattering, might be found in kaon photoproduction since they may couple strongly to  $K\Lambda$  and  $K\Sigma$  channels.

At photon laboratory energies from the kaon photoproduction threshold of  $\sqrt{s} = 1.61$  GeV to about 2.5 GeV, the isobar model is most widely used for extracting  $N^*$  parameters from the kaon photoproduction data [3–8]. This model is based on an effective Lagrangian approach in which a number of tree diagrams are evaluated with coupling constants partly fixed from independent hadronic and electromagnetic data. Although the isobar models describe the existing kaon photoproduction data fairly well, multi-step or coupled-channel (CC) effects due to intermediate  $\pi N$  states are ignored. The sequence  $\gamma N \rightarrow \pi N \rightarrow KY$  in kaon photoproduction can be substantial, since  $\gamma N \rightarrow \pi N$  amplitudes are much greater than the direct  $\gamma N \rightarrow KY$  amplitudes. If this is indeed the case, the  $N^*$  parameters obtained from one-step isobar models can not be directly compared with the predictions from existing hadron models. The importance of the final-state interaction(FSI) in interpreting the  $\Delta$  resonant parameters extracted from  $\gamma N \rightarrow \pi N$  data has been demonstrated in Ref. [9]. In this work, we investigate the same problem concerning the role of CC final state interactions in kaon photoproduction.

Among existing studies of kaon photoproduction, coupled-channel effects have been investigated using two approaches. Kaiser *et al.* [10] applied a coupled-channel approach with chiral SU(3) dynamics to investigate pion- and photon-induced meson production near the  $KY$  threshold. Although their recent results [11] include p-wave multipoles, and thus reproduce data slightly above the threshold region, their chiral SU(3) dynamics model can not provide the higher partial waves that are important in describing the data at higher energies. A similar approach has also been taken in Ref. [12].

The second CC approach was developed by Feuster and Mosel [13]. They used a  $K$ -matrix method to investigate photon- and meson-induced reactions, including  $\gamma p \rightarrow K^+\Lambda$ . In the  $K$ -matrix approach, all intermediate states are put on-shell and hence the important off-shell dynamical effects can not be accounted for explicitly. The advantage of their approach is its numerical sim-

plicity in handling a large number of coupled channels. However, the extracted  $N^*$  parameters may suffer from the difficulties in interpreting them in terms of extant hadron models, such as the constituent quark model.

In this paper, we present a dynamical CC model in which the meson-baryon off-shell interactions are defined in terms of effective Lagrangians. This is achieved by a direct extension of the existing dynamical models [9,14–16] for pion photoproduction to include  $KY$  channels. We follow the approach developed by Sato and Lee [9]. In this first attempt, we do however need to make several simplifications since it is a rather complex task to deal simultaneously with the meson-baryon and photon-baryon intertwined CC problems. First, we adopt an existing isobar model developed earlier by Williams, Ji and Cotanch (WJC) [5] as initial input for the direct  $\gamma p \rightarrow K^+ \Lambda$  process. This fixes the number of  $N^*$  to be considered and the leading tree-diagrams associated with strange particles. Second, we use the  $\gamma N \rightarrow \pi N$  and  $\pi N \rightarrow \pi N$  partial-wave amplitudes from the VPI partial-wave analysis [17,18] to define the amplitudes associated with the  $\pi N$  channel. This drastically reduces the amount of data we have to confront in the coupled-channel approach. However, the strong interaction matrix elements of  $KY \rightarrow KY$  and  $\pi N \rightarrow KY$  transition operators are derived rigorously from effective Lagrangians using the unitary transformation method of Ref. [9]. This derivation marks our major differences with Kaiser *et al.* [10] since we include all relevant higher partial waves and our approach is applicable at all energies. We solve the resulting CC equations with numerical precision to account for the meson-baryon off-shell interactions. The dynamical content of our approach is clearly very different from the  $K$ -matrix model of Feuster and Mosel [13].

Our CC approach is defined by the starting Lagrangian and by the several approximations such as the Sato-Lee unitary transformation and a three-dimensional reduction of the Bethe-Salpeter equation. Such approximations have been pursued successfully by numerous authors in order to solve difficult strong interaction problems starting from relativistic field theory. Lagrangian-based dynamics differs considerably from models motivated by the  $S$ - or  $K$ -matrix approach based on tree-diagrams, in which the dynamics is partly defined by postulating crossing symmetry [19]. While S-matrix plus tree-diagram approaches can be a very useful working tool, no solid proof exists that crossing symmetry can be derived “exactly” from relativistic quantum field theory. The best effort is a perturbative derivation in a simple model, such as presented in Bjorken and Drell. Thus, our approach is not expected to respect crossing symmetry, although the driving terms of the employed coupled-channel scattering equations can be made to have crossing symmetry. Compared with the previous models based on tree-diagrams supplemented by crossing symmetry [5,7,26], the coupled-channel approach can satisfy “dynamically” the multi-channel unitarity condition. The CC approach offers the advantage of including strong dynamics for both kaon photoproduction and kaon radiative

decays, while also incorporating cusp structure due to channel coupling, which is not described by tree-diagram based theories. Therefore, there are advantages to the CC approach that we believe out-weigh the desire for a crossing symmetric theory.

## 2 Coupled-channel approach

A coupled-channel framework for studying kaon photoproduction can be obtained straightforwardly by generalizing the dynamical approach developed by Sato and Lee [9] in their investigation of  $\pi N$  scattering and pion photoproduction. By adding the  $KY$  channel and appropriate  $N^*$  states to their formalism, one can show that the collision matrix,  $A_{KY,\gamma N}$ , of the  $\gamma N \rightarrow KY$  reaction can be written in operator form as

$$A_{KY,\gamma N} = R_{KY,\gamma N} + a_{KY,\gamma N}. \quad (1)$$

Here  $R_{KY,\gamma N}$  denotes the resonant part (to be specified later), and the non-resonant part  $a_{KY,\gamma N}$  is defined by

$$a_{KY,\gamma N} = b_{KY,\gamma N} + \sum_{K'Y'} t_{KY,K'Y'} G_{K'Y'}^{(+)} b_{K'Y',\gamma N} + \sum_{\pi N} t_{KY,\pi N} G_{\pi N}^{(+)} b_{\pi N,\gamma N}, \quad (2)$$

where  $G_{\alpha}^{(+)}$  is the meson-baryon propagator for channel  $\alpha$ . Here  $b_{KY,\gamma N}$  and  $b_{\pi N,\gamma N}$  are the nonresonant photoproduction operators for  $KY$  and  $\pi N$  respectively. The scattering operators  $t_{KY,K'Y'}$  and  $t_{KY,\pi N}$  describe the nonresonant parts of the final  $KY \rightarrow K'Y'$  and  $\pi N \rightarrow KY$  transitions, respectively. Obviously, the third term of Eq. (2) contains the coupled-channel effects due to the intermediate  $\pi N$  channel.

To see the dynamical feature of our CC approach, we now combine the resonant term  $R_{KY,\gamma N}$  with the nonresonant operator  $b_{KY,\gamma N}$  and define  $B_{KY,\gamma N} \equiv R_{KY,\gamma N} + b_{KY,\gamma N}$ . Eqs. (1)-(2) then become

$$A_{KY,\gamma N} = B_{KY,\gamma N} + \sum_{K'Y'} t_{KY,K'Y'} G_{K'Y'}^{(+)} b_{K'Y',\gamma N} + \sum_{\pi N} t_{KY,\pi N} G_{\pi N}^{(+)} b_{\pi N,\gamma N}. \quad (3)$$

The nonresonant meson-baryon transition operators  $t_{KY,KY}$  and  $t_{KY,\pi N}$  are defined by the following CC equations:

$$t_{KY_f, KY_i} = v_{KY_f, KY_i} + \sum_{KY} v_{KY_f, KY} G_{KY}^{(+)} t_{KY, KY_i} + \sum_{\pi N} v_{KY_f, \pi N} G_{\pi N}^{(+)} t_{\pi N, KY_i}, \quad (4)$$

$$t_{KY_f, \pi N_i} = v_{KY_f, \pi N_i} + \sum_{KY} v_{KY_f, KY} G_{KY}^{(+)} t_{KY, \pi N_i} + \sum_{\pi N} v_{KY_f, \pi N} G_{\pi N}^{(+)} t_{\pi N, \pi N_i}. \quad (5)$$

The above equations define the off-shell scattering amplitudes. Clearly, the amplitudes  $t_{KY, K'Y'}$  and  $t_{KY, \pi N}$ , which are needed to evaluate the second and third terms of Eq. (3), can be obtained from solving Eqs. (4)-(5) if the potentials  $v_{KY, K'Y'}$  and  $v_{KY, \pi N}$  and the nonresonant  $\pi N$  amplitude  $t_{\pi N, \pi N}$  can be calculated from a model. We now note that if the last two terms in the right-hand-side of Eq. (3) are neglected, our CC model reduces to those previously developed isobar models for which  $A_{KY, \gamma N} = B_{KY, \gamma N}$ . In that limit, the resonances are then included in the  $R$  term.

The nonresonant meson-baryon  $t$ -matrix defined by Eqs. (4)-(5) is only part of the full meson-baryon scattering  $T$ -matrix. The  $N^*$  excitations must be included. By extending the  $\pi N$  scattering formulation of Ref. [9] to include the  $KY$  channel, one can show that the full meson-baryon scattering amplitude can be written as

$$T_{\alpha, \beta}(E) = t_{\alpha, \beta}(E) + t_{\alpha, \beta}^R(E), \quad (6)$$

where  $\alpha, \beta = \pi N, KY$ . The nonresonant amplitudes  $t_{\alpha, \beta}$  are identical to those in Eqs. (4)-(5). The resonant term at resonant energy  $E_{N^*}$  can be written in the familiar Breit-Wigner form (after performing a proper diagonalization in the  $N^*$  channel space)

$$t_{\alpha, \beta}^R(E) = \sum_{N^*} \frac{\bar{\Gamma}_{N^*, \alpha}^* \bar{\Gamma}_{N^*, \beta}}{E - E_{N^*} + \frac{i}{2} \Gamma_{N^*}^{(tot)}}, \quad (7)$$

with the total width

$$\Gamma_{N^*}^{(tot)} = \sum_{\alpha} |\bar{\Gamma}_{N^*, \alpha}|^2. \quad (8)$$

In the above equations,  $\bar{\Gamma}_{N^*, \alpha}$  describes the decay of an  $N^*$  resonance into a meson-baryon channel  $\alpha$ . Eqs. (6)-(8) will be the starting point for developing a strategy for using the empirical  $\pi N$  scattering amplitudes to solve Eqs. (4)-(5).

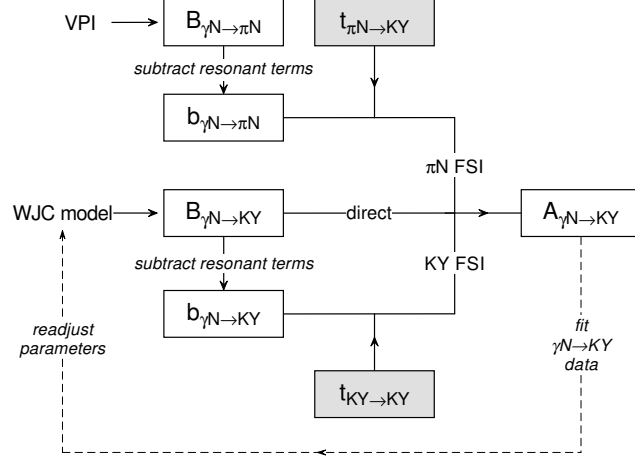


Fig. 1. Flow chart of our CC approach for kaon photoproduction. See the text for a description.

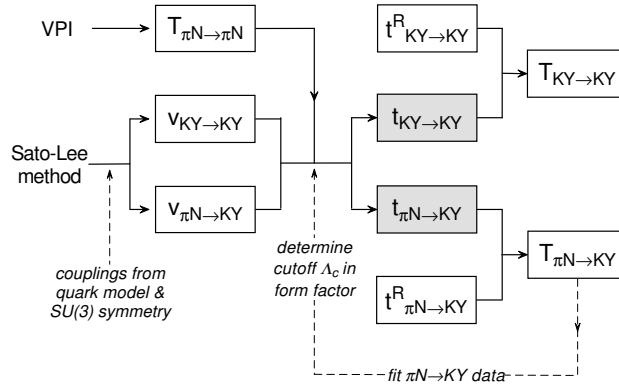


Fig. 2. Flow chart for the construction of the CC/FSI meson-baryon  $t$ -matrices. See the text for a description.

### 3 Simplifications

One way to approach the coupled-channel equations presented in the previous section is to use effective Lagrangians to construct the photoproduction operators  $b_{KY,\gamma N}$  and  $b_{\pi N,\gamma N}$ , and meson-baryon potentials  $v_{\alpha,\beta}$ . Then one could attempt to solve the full  $T$ -matrix equations consistently as done in Ref. [9] for pion photoproduction. This program is too difficult and we therefore make some simplifications in order to first gauge the role of the  $\pi N$  channels in kaon photoproduction. The procedures used in this paper are outlined in Figures 1 and 2.

As indicated in Figure 1, we take the isobar model developed by Williams, Ji and Cotanch (WJC) [5] to describe the direct kaon photoproduction. The WJC model contains both the resonant and nonresonant amplitudes, but does not include the meson-baryon final state interactions. Thus, we can identify the amplitude generated from this isobar model as  $B_{KY,\gamma N}$  in Eq. (3). The nonresonant term  $b_{KY,\gamma N}$  needed for evaluating Eq. (2) can then be obtained from

$$b_{KY,\gamma N} = [B_{KY,\gamma N}]_{WJC} - [R_{KY,\gamma N}]_{WJC} \quad (9)$$

where the resonant part  $[R_{KY,\gamma N}]_{WJC}$  is also from the WJC model. The “subtract resonance term” procedure Eq. (9) is indicated in the lower left part of Fig. 1.

Turning to the upper part of Figure 1, we do not compute the amplitude of the  $\gamma N \rightarrow \pi N$  process—that is a complicated CC problem by itself. Instead, we start with the VPI partial-wave amplitudes for pion photoproduction [18]. We then define the nonresonant part of pion photoproduction amplitude by subtraction

$$b_{\pi N,\gamma N} = [B_{\pi N,\gamma N}]_{VPI} - R_{\pi N,\gamma N}, \quad (10)$$

where the resonant amplitude is calculated from

$$R_{\pi N,\gamma N}(E) = \sum_{N^*} \frac{\bar{\Gamma}_{N^*,\pi N}^* \bar{\Gamma}_{N^*,\gamma N}}{E - E_{N^*} + \frac{i}{2}\Gamma_{N^*}^{(tot)}}. \quad (11)$$

The partial decay widths  $\bar{\Gamma}_{N^*,\gamma N}$  and  $\bar{\Gamma}_{N^*,\pi N}$  and the total widths  $\Gamma_{N^*}^{(tot)}$  can be calculated from the parameters listed by the Particle Data Group (PDG).

Eqs. (9) and (10) only define the on-shell matrix elements of the nonresonant photoproduction amplitudes. To evaluate the second and the third FSI terms in Eq. (3), we need to define their off-shell behavior. For simplicity, we set

$$b_{\alpha,\gamma N}(q, k; E) = b_{\alpha,\gamma N}(q_0, k; E) \cdot \frac{F(q)}{F(q_0)}, \quad (12)$$

where  $\alpha = KY$  and  $\pi N$ ,  $k$  and  $q_0$  are the on-shell photon and meson momenta fixed by the total energy  $E$ ,  $q$  is the desired off-shell value, and  $F(q)$  is a form factor to be defined later.

We now introduce a procedure to calculate the nonresonant meson-baryon amplitudes  $t_{KY,K'Y'}$  and  $t_{KY,\pi N}$ , which are shown as shaded boxes in Fig. 1.

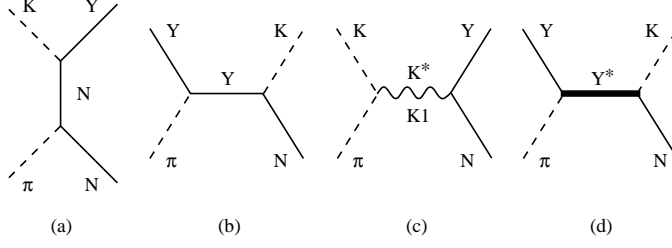


Fig. 3. Graphical representation of the potentials in  $\pi N \rightarrow KY$ . (a) direct nucleon pole  $v_{ND}$ , (b) hyperon exchange  $v_{YE}$ , (c) strange vector meson exchange  $v_{K^*}$ , and (d) hyperon resonance exchange  $v_{Y^*}$ .

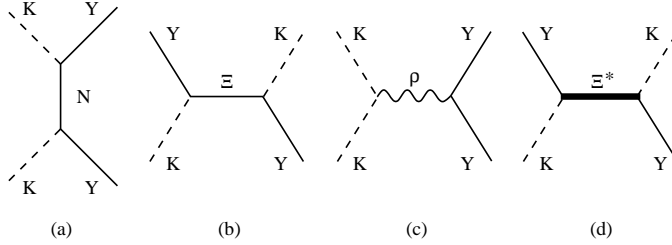


Fig. 4. Graphical representation of the potentials in  $KY \rightarrow KY$ . (a) direct nucleon pole  $v_{ND}$ , (b)  $\Xi$  exchange  $v_{XE}$ , (c) vector meson exchange  $v_{\rho}$ , and (d)  $\Xi$  resonance exchange  $v_{\Xi^*}$ .

The procedure for obtaining these transition amplitudes is outlined in Fig. 2. We again start with the VPI amplitude. By using Eqs. (6)-(8), the on-shell nonresonant part of  $\pi N$  amplitude  $t_{\pi N, \pi N}$  is then defined by

$$t_{\pi N, \pi N} = [T_{\pi N, \pi N}]_{VPI} - t_{\pi N, \pi N}^R, \quad (13)$$

where the resonant term  $t_{\pi N, \pi N}^R$ , defined by Eq. (7), can be calculated using the resonant parameters listed by PDG. We then use the same off-shell extrapolation defined by Eq. (12) to define the half-off-shell  $\pi N$  t-matrix which is needed to evaluate the matrix element of the second term of Eq. (5).

With the nonresonant  $t_{\pi N, \pi N}$  defined by the above procedure, Eqs. (4)-(5) can be solved by constructing the potentials  $v_{KY, KY}$  and  $v_{KY, \pi N}$ . Here we use the unitary transformation method of Ref. [9]. The considered potentials are illustrated in Figs. 3 and 4. To solve the coupled equations (4)-(5), the meson-baryon potentials must also be regularized by form factors. For simplicity, a form factor  $F(\mathbf{q}) = (\frac{\Lambda_c^2}{\Lambda_c^2 + \mathbf{q}^2})^2$  is used to regularize all vertices in Figs. 3 and 4, where  $\mathbf{q}$  is the momentum of the external meson in the center-of-mass frame.

To minimize the number of free parameters in this calculation, we fix most of the couplings in Figs. 3 and 4 by using either the known PDG values [20], or from the predictions of SU(3) flavor symmetry [21] or constituent quark models [22,23]. The coupling strengths of the terms involving  $\Xi$  and  $\Xi^*$  are not known and therefore are not included in this exploratory investigation.



This of course should be improved in later studies. To further simplify the calculation, the form factor  $F(q)$ , used in defining the off-shell behavior of the nonresonant photoproduction and  $t_{\pi N, \pi N}$ , is assumed to be the same as that for regularizing the potentials  $v_{KY, KY}$  and  $v_{KY, \pi N}$ . Thus, only one cutoff  $\Lambda_c$  needs to be determined.

## 4 Results

We start with the WJC model and hence the considered resonances and all coupling strengths are fixed, as listed in the third column of Table 1. The only parameter in our CC model is the cutoff  $\Lambda_c$  of the form factors which regularize  $b_{\pi N, \gamma N}$ ,  $b_{KY, \gamma N}$ ,  $t_{\pi N, \pi N}$ , and potentials  $v_{KY, KY}$  and  $v_{KY, \pi N}$ , as described in Section 3. We determine this parameter by fitting the  $\pi^- p \rightarrow K^0 \Lambda$  data. This fit is done by first solving Eqs. (4)-(5) to obtain the nonresonant amplitude  $t_{K\Lambda, \pi N}$ . The resonant part of this reaction is calculated from using Eq. (7) and the resonant parameters listed by PDG. We find that the total cross section data of  $\pi^- p \rightarrow K^0 \Lambda$  can be fitted by setting  $\Lambda_c = 680$  (MeV/c). This procedure then fixes the nonresonant meson-baryon amplitudes  $t_{KY, K'Y'}$  and  $t_{KY, \pi N}$  that are needed to evaluate the FSI effects on the photoproduction amplitude using Eq. (3).

In Figure 5, we illustrate the predicted FSI effects on the total cross sections of  $\gamma p \rightarrow K^+ \Lambda$ . Four curves are shown: (1) the direct photoproduction calculated using the WJC model,  $B_{K\Lambda}$ ; (2) the direct production plus the  $K\Lambda$  FSI effects,  $B_{K\Lambda} + t_{K\Lambda, K\Lambda} G_{K\Lambda}^{(+)} b_{K\Lambda}$ ; (3) the direct production plus the  $\pi N$  FSI effects,  $B_{K\Lambda} + t_{K\Lambda, \pi N} G_{\pi N}^{(+)} b_{\pi N}$ ; (4) the direct results plus both the  $K\Lambda$  and  $\pi N$  FSI effects, i.e., our full CC results  $A_{K\Lambda}$ . We also compare these results with the SAPHIR data [24]. Note that the WJC model was developed before the SAPHIR measurement and hence their original fit (dashed curve) deviates from these recent data.

In Figure 5, we see significant differences up to 20% of the total cross sections with the  $\pi N$  FSI (third term of Eq. (3)) turned on and off. Clearly, the CC effects due to the  $\pi N$  channels make quite a sizable contribution to kaon photoproduction and should be included in any kaon photoproduction calculation. Further examination reveals that the major CC effects are from the s-wave  $E_{0+}$  multipole. In contrast, the  $K\Lambda$  FSI effect (second term of Eq. (3)) is quite small.

Our full results (solid curve in Fig. 5) based on the WJC parameters deviate from the experimental data. We find that the data can not be reproduced by only changing the original WJC parameters. Here we emphasize that WJC published their predictions prior to the SAPHIR measurements. In trying to

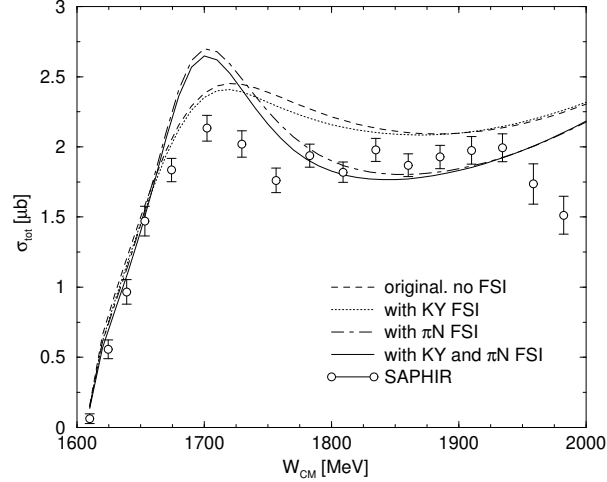


Fig. 5. Total cross sections for  $\gamma p \rightarrow K^+ \Lambda$  calculated using the CC approach with the original WJC coupling parameters. The curves are for the direct production  $B_{K\Lambda}$  (dashed line),  $B_{K\Lambda}$  plus  $K\Lambda$  FSI effects (dotted),  $B_{K\Lambda}$  plus  $\pi N$  FSI effects (dash-dotted), and full CC results  $A_{K\Lambda}$  including  $K\Lambda$  and  $\pi N$  FSI (solid). Results are compared with the SAPHIR data [24].

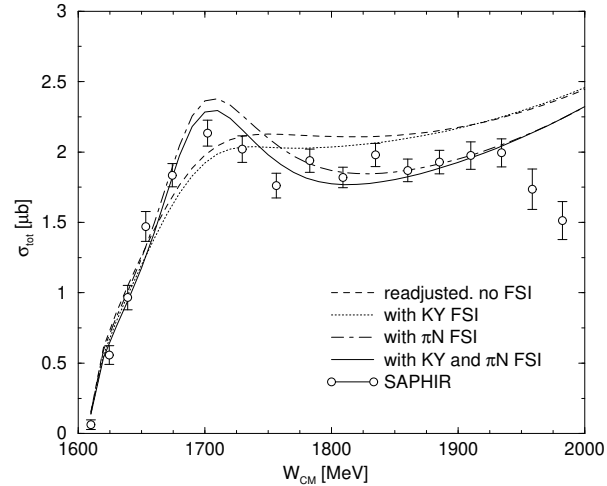


Fig. 6. Total cross sections for  $\gamma p \rightarrow K^+ \Lambda$  calculated using the CC approach with our readjusted coupling parameters. Curves and data as in Fig. 5.

fit this new data set, containing both differential and total cross sections, we fail to reproduce the high energy ( $W > 1950$  MeV) part. This failure is likely due to our lack of resonances with mass around 1800 to 1900 MeV. It has been shown [25] that good agreement with SAPHIR data is obtained if one introduces two spin-3/2 resonances  $N^*(1720)$  and  $\Lambda^*(1890)$ , provided off-shell effects are included [26]. However, including those two spin-3/2 resonances, with off-shell dynamics, requires 3 extra free parameters per resonance. Our CC study aims to delineate the role of FSI and we wish to keep the number of free parameters as small as possible. That is why we have not yet introduced the requisite spin-3/2 resonances, but only spin-1/2 resonances. One of these

Table 1

Original fit parameters in the WJC model [5] and our readjusted values. The resonance couplings are the products of photon and hadronic couplings.

Particle	Coupling	WJC value	Readjusted value
$\Lambda$	$\frac{g_{K\Lambda N}}{\sqrt{4\pi}}$	-2.377	-2.377
$\Sigma^0$	$\frac{g_{K\Sigma N}}{\sqrt{4\pi}}$	0.222	0.404
$K^*$	$\frac{G_{K^*}^V}{\sqrt{4\pi}}$	-0.162	-0.162
	$\frac{G_{K^*}^T}{4\pi}$	0.078	0.078
$K1$	$\frac{G_{K1}^V}{4\pi}$	0.019	0.019
	$\frac{G_{K1}^T}{4\pi}$	0.173	0.173
$N^*(1535)$	$\frac{G_{N3}}{\sqrt{4\pi}}$	0	0.030
$N^*(1650)$	$\frac{G_{N4}}{\sqrt{4\pi}}$	-0.044	-0.025
$N^*(1710)$	$\frac{G_{N6}}{\sqrt{4\pi}}$	-0.064	-0.064
$\Lambda^*(1405)$	$\frac{G_{L1}}{\sqrt{4\pi}}$	-0.073	-0.073
$\Lambda^*(1810)$	$\frac{G_{L5}}{\sqrt{4\pi}}$	0	0.125

spin-1/2 resonances that we do include, the  $\Lambda^*(1810)$ , is of some help in the relevant 1800 to 1900 MeV mass range. We also note that a small contribution from the  $N^*(1535)$  also improves the fit.

The extracted coupling constants (Table 1, last column) show that only two of the original WJC couplings get modified. The curve corresponding to the parameter changes is depicted in Fig. 6, where we also show the results of the FSI decomposed as in Fig. 5. Comparison between Figs. 5 and 6 make clear that the numerical results for the FSI depend on the resonance content of the reaction mechanism. However, this dependence is very smooth in the case of the two configurations considered here and does not alter the general trends nor the importance of the FSI effects.

## 5 Conclusions

In this work we do not aim for an accurate reproduction of the data of kaon photoproduction. We rather focus on the coupled-channel effects on this reaction. The major conclusion from this study is that the  $\pi N$  channels make significant contributions through the coupled-channel mechanism and must be

included in a proper calculation for kaon photoproduction reactions.

Our approach, based on an extension of the dynamical model of Ref. [9], will be the basis for future investigations. In particular, the  $K\Sigma$  channels must be included in a more complete study of kaon electromagnetic production, which is currently in progress. It is especially interesting to study the  $K\Sigma$  threshold effects (e.g., cusps at  $K\Sigma$  threshold) in a CC calculation and their effect on spin observables. In addition, more channels, such as  $\eta N$ ,  $\pi\Delta$  and  $\rho N$ , must be included in a complete coupled-channel calculation.

## Acknowledgements

The authors would like to thank S.A. Dytman, R. Schumacher, and S.N. Yang for helpful discussions. W.-T. C. is grateful to ANL and Saclay for the hospitality extended to him during his visits. This work was supported in parts by the U.S. National Science Foundation (PHY-9514885 and PHY-9970775), the National Science Council of ROC under grant No. NSC89-2112-M002-078, a University of Pittsburgh Andrew Mellon Predoctoral Fellowship, and U.S. DOE Nuclear Physics Division(Contract No. W-31-109-ENG).

## References

- [1] S. Capstick and W. Roberts, Nucl. Phys. 45 Suppl. 2 (2000) 5241.
- [2] R. Bijker, F. Iachello, and A. Leviatan, Prog. Part. Nucl. Phys. 284 (2000) 89.
- [3] R.A. Adelseck, C. Bennhold, and L.E. Wright, Phys. Rev. C32 (1985) 1681.
- [4] R.A. Adelseck and B. Saghai, Phys. Rev. C42 (1990) 108.
- [5] R.A. Williams, C.R. Ji, and S.R. Cotanch, Phys. Rev. C46 (1992) 1617.
- [6] T. Mart, C. Bennhold, and C.E. Hyde-Wright, Phys. Rev. C51 (1995) 1074.
- [7] J.C. David, C. Fayard, G.H. Lamot, and B. Saghai, Phys. Rev. C53 (1996) 2613.
- [8] S. S. Hsiao, D.H. Lu, and S.N. Yang, Phys. Rev. C61 (2000) 068201.
- [9] T. Sato and T.-S.H. Lee, Phys. Rev. C54 (1996) 2660.
- [10] N. Kaiser, T. Waas, and W. Weise, Nucl. Phys. A612 (1997) 297.
- [11] J. Caro Ramon, N. Kaiser, S. Wetzell, and W. Weise, Nucl. Phys. A672 (2000) 249.
- [12] J.A. Oller, E. Oset, and A. Ramos, Prog. Part. Nucl. Phys. 45 (2000) 157.

- [13] T. Feuster and U. Mosel, Phys. Rev. C59 (1999) 460.
- [14] S.N. Yang, J. Phys. G 11 (1985) L205.
- [15] H. Tanabe and K. Ohta, Phys. Rev. C31 (1985) 1876.
- [16] S. Nozawa, B. Blankleider, and T.-S.H. Lee, Nucl. Phys. A513 (1990) 459.
- [17] R.A. Arndt, I.I. Strakovsky, R.L. Workman, and M.M. Pavan, Phys. Rev. C52 (1995) 2120.
- [18] R.A. Arndt, I.I. Strakovsky, and R.L. Workman, Phys. Rev. C53 (1996) 430.
- [19] F.M. Renard and Y. Renard, Nuovo Cim. 55A (1968) 631; C.R. Ji, and S.R. Cotanch, Phys. Rev. C38 (1988) 2691; S.R. Cotanch, R.A. Williams, and C.R. Ji, Phys. Scripta 48 (1993) 217, and references therein.
- [20] D.E. Groom *et al.*, Particle Data Group, Eur. Phys. J. C15 (2000) 1.
- [21] V.G.J. Stoks and T.A. Rijken, Nucl. Phys. A613 (1997) 311.
- [22] S. Capstick and W. Roberts, Phys. Rev. D58 (1998) 074011.
- [23] R. Koniuk and N. Isgur, Phys. Rev. D21 (1980) 1868.
- [24] M.Q. Tran *et al.*, Phys. Lett. B445 (1998) 20.
- [25] B. Saghai, Proceedings of the *Workshop on Hypernuclear Physics with Electromagnetic Probes (HJLAB99)*, Hampton, Virginia, 2-4 Dec. 1999, eds. O.K. Baker and O. Hashimoto, *under press*.
- [26] T. Mizutani, C. Fayard, G.H. Lamot, and B. Saghai, Phys. Rev. C58 (1998) 75.